Determination of and evidence for non-core-shell structure of particles containing black carbon using the Single-Particle Soot Photometer (SP2)

Arthur J. Sedlacek III,[1] Ernie R. Lewis,[1] Lawrence Kleinman,[1] Jianzhong Xu,[2] and Qi Zhang[2]

Received 10 January 2012; revised 14 February 2012; accepted 21 February 2012; published 17 March 2012.

[1] The large uncertainty associated with black carbon (BC) direct forcing is due, in part, to the dependence of light absorption of BC-containing particles on the position of the BC within the particle. It is predicted that this absorption will be greatest for an idealized core-shell configuration in which the BC is a sphere at the center of the particle whereas much less absorption should be observed for particles in which the BC is located near or on the surface. Such microphysical information on BC-containing particles has previously been provided only by labor-intensive microscopy techniques, thus often requiring that climate modelers make assumptions about the location of the BC within the particle that are based more on mathematical simplicity than physical reality. The present paper describes a novel analysis method that utilizes the temporal behavior of the scattering and incandescence signals from individual particles containing refractory BC (rBC) measured by the Single-Particle Soot Photometer (SP2) to distinguish particles with rBC near the surface from those that have structures more closely resembling the core-shell configuration. This approach permits collection of a high-time-resolution data set of the fraction of rBC-containing particles with rBC near the surface. By application of this method to a plume containing tracers for biomass burning, it was determined that this fraction was greater than 60%. Such a data set will not only provide previously unavailable information to the climate modeling community, allowing greater accuracy in calculating rBC radiative forcing, but also will yield insight into aerosol processes.
Citation: Sedlacek, A. J., III, E. R. Lewis, L. Kleinman, J. Xu, and Q. Zhang (2012), Determination of and evidence for non-core-shell structure of particles containing black carbon using the Single-Particle Soot Photometer (SP2), *Geophys. Res. Lett.*, *39*, L06802, doi:10.1029/2012GL050905.

1. Introduction

[2] Despite research focused at reducing the uncertainty associated with radiative forcing due to particles containing black carbon (BC), the complex aging and structural behavior of such particles has made this goal difficult to achieve [e.g., *Forster et al.*, 2007; *Ramanathan and Carmichael*, 2008]. Key reasons for this difficulty are the dependences of the particle optical properties on the morphology of the BC itself and on the position of the BC within the particle. For example, a nascent (fractal) BC aggregate consisting of a large number of smaller spherules, all of which can participate in light absorption, will exhibit a larger mass-absorption cross-section than the collapsed form of the aggregate in which screening will result in fewer spherules interacting with the incident light [*Bond and Bergstrom*, 2006]. The existence of a coating on BC can result in increased mass-absorption cross-section through a lensing effect [*Ackerman and Toon*, 1981; *Jacobson*, 2001] that has been confirmed in several controlled laboratory experiments, with the increase sometimes approaching 100% or more relative to uncoated BC [*Cross et al.*, 2010, and references therein]. Finally, the positioning of the BC within the particle can also influence the amount of light absorption [*Fuller et al.*, 1999, and references therein], as greater absorption is expected for particles with the BC surrounded by a uniform non-refractory coating than for those particles for which the BC is near the surface.

[3] Whereas information can be collected to identify coating composition, and BC size and mass distributions can be routinely measured, the position of the BC within the particle and the morphological state of the BC itself are difficult to determine, and generally available only through labor-intensive microscopy-based studies [e.g., *Adachi et al.*, 2010; *Pósfai and Buseck*, 2010, and references therein]. In the absence of structural information on particles containing BC, climate modelers have chosen to make assumptions about the location of the BC within the particle that are based more on mathematical simplicity than physical reality. The present paper describes a novel analysis technique that can distinguish those BC-containing particles for which BC is located near the surface from those that have structures more closely resembling the idealized core-shell configuration by examining the temporal behavior of the scattering and incandescence signals collected from individual particles using the Single-Particle Soot Photometer (SP2). Given the inconsistencies in the aerosol literature regarding terminology, e.g., BC, soot, light-absorbing carbon [*Bond and Bergstrom*, 2006], we adopt the nomenclature advocated by *Schwarz et al.* [2010] and widely used by the SP2 community that the SP2 measures refractory black carbon (rBC) defined operationally by its incandescence temperature.

2. Experiment

[4] During the summer of 2011, a two-month field campaign was conducted at Brookhaven National Laboratory on Long Island, NY to study the evolution of aerosol microphysical

[1]Atmospheric Science Division, Brookhaven National Laboratory, Upton, New York, USA.
[2]Department of Environmental Toxicology, University of California, Davis, California, USA.

0094-8276/12/2012GL050905

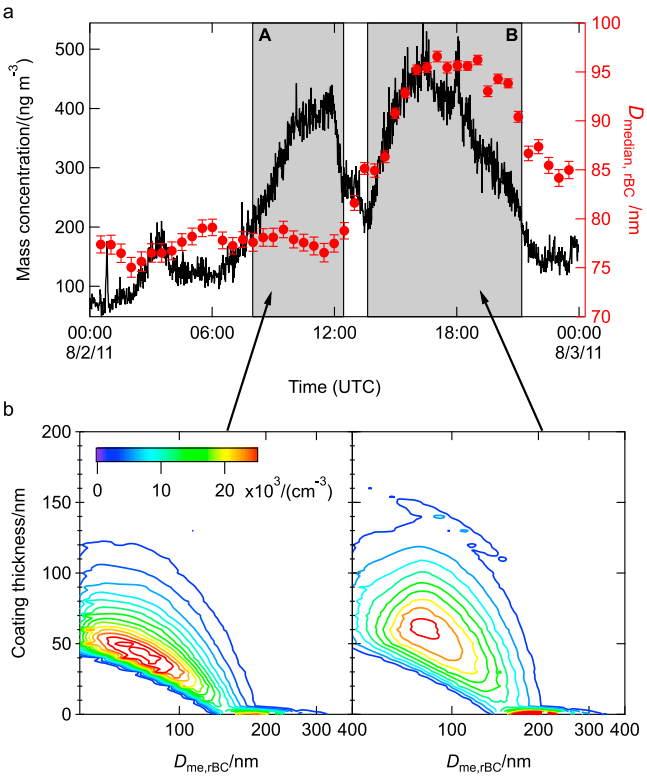

Figure 1. (a) Mass concentration of rBC (black line) determined by incandescence and median diameter of rBC, $D_{\mathrm{median,rBC}}$, integrated over 30-min intervals (red dots) with error bars denoting one standard deviation. Shaded regions delineate episodes A and B. (b) Coating thickness of rBC-containing particles determined by optical diameter method integrated over episode A and B as a function of rBC mass-equivalent diameter, $D_{\mathrm{me,rBC}}$.

and optical properties. As a detailed description of this campaign will be the subject of a forthcoming paper, only aspects relevant to the present discussion are highlighted here. The measurement site (40.871°N, 72.89°W) was located 80 km east of New York City and situated in an area characterized by pine-oak forests and small urban townships, with the Atlantic Ocean 25 km to the south and Long Island Sound (an estuary of the Atlantic Ocean) 16 km to the north. As part of the instrumentation suite, a Single-Particle Soot Photometer (SP2; Droplet Measurement Technologies) and a High Resolution Time-of-Flight Aerosol Mass Spectrometer (HR-ToF-AMS; Aerodyne) were deployed to examine the evolution of the mixing state of rBC-containing particles.

[5] The SP2 measures both scattering and incandescence from individual particles containing rBC that are illuminated with a 1064 nm (near-IR) laser beam [*Schwarz et al.*, 2006; *Moteki and Kondo*, 2008; *Subramanian et al.*, 2010]. For a uniformly coated rBC particle the energy absorbed by rBC dissipates first as latent heat through evaporation of the coating and then through incandescence of rBC. Determination of incandescence signals that originate solely from rBC is realized through consideration of color temperature using broadband and narrowband filters [*Schwarz et al.*, 2006; *Moteki and Kondo*, 2007]. The incandescence signal can probe particles with mass-equivalent diameter of rBC, $D_{\mathrm{me,rBC}}$, from nominally 65–600 nm, but the limited range of the optical diameters determined from the scattering signal (~165–350 nm for the present instrument) ultimately determines those particles for which mixing state analysis can be performed.

[6] The amount of non-refractory material associated with an rBC-containing particle can be estimated using one of two methods. The first, referred to here as the optical diameter method, calculates a coating thickness as the difference between the optical diameter determined from the scattering signal and $D_{\mathrm{me,rBC}}$ determined from the incandescence signal (which is directly proportional to the rBC mass). This coating thickness is that which would occur if the coating were uniformly distributed around the rBC. Determination of particle diameter from the scattering signal requires assumptions about the refractive index, the particle composition (which is typically unknown), and particle structure. The second approach, the lagtime method, estimates the amount of non-refractory material using the proxy of lagtime, $\Delta\tau$: the time of the peak of the incandescence signal minus the time of the peak of the scattering signal [*Schwarz et al.*, 2006; *Moteki and Kondo*, 2007; *Subramanian et al.*, 2010]. This lagtime increases with increased amount of non-refractory material, although the complex behavior of heat transfer and evaporation and the lack of knowledge of the thermo-chemical and thermo-physical properties of the coating material preclude a quantitative determination of the thickness based on lagtime.

3. Results and Discussion

[7] Of particular interest to the present discussion are two episodes sampled on August 2, 2011 in which large increases in the mass concentration of rBC were observed (Figure 1a). The greatest concentrations occurred near 12:00 UTC for episode A and near 16:00 UTC for episode B (local time is 4 hours behind UTC). The wind direction remained out of the west during the course of these two events (246 ± 53° for episode A and 272 ± 24° for episode B), with light and variable winds less than 1 m s^{-1} for episode A, which had increased to 2–2.5 m s^{-1} for episode B.

[8] No increase in the median rBC mass-equivalent diameter (averaged over 30 minute intervals), $D_{\mathrm{median,rBC}}$, was apparent in episode A, whereas there was a pronounced increase in $D_{\mathrm{median,rBC}}$ from less than 80 nm to near 100 nm at the peak of episode B (Figure 1a). Episode B was characterized by rBC-containing particles with much greater coating thicknesses as calculated using the optical diameter method (Figure 1b). The coating thickness for particles containing rBC with $D_{\mathrm{me,rBC}}$ = 80 nm in episode B exhibited high correlation with the organic aerosol mass concentration measured by the HR-ToF-AMS, although not with the mass concentrations of sulfate or nitrate (Figure 2). Both this coating thickness and the organic aerosol mass concentration, together with the corresponding increase in O:C ratio as well as change in the bulk composition of organic aerosols determined from the HR-ToF-AMS (Figure 2) and the observed increase in $D_{\mathrm{median,rBC}}$ for rBC (Figure 1), indicate advection of a new air mass into the measurement site and strongly suggest that the rBC coating material is organic.

[9] Particles in episodes A and B also exhibit different lagtime behavior with respect to $D_{\mathrm{me,rBC}}$ (Figure 3). Lagtimes for episode A (Figure 3a) are bimodal, with one mode resulting from those particles that contain large amounts of

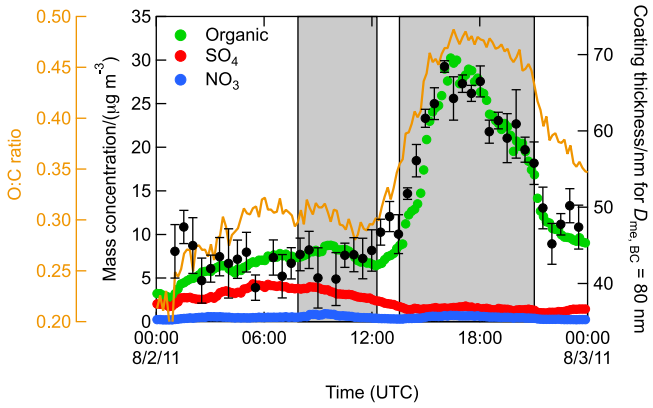

Figure 2. Aerosol mass concentration of organics (green), SO_4 (red), and NO_3 (blue), with O:C ratio (gold), all determined by the High Resolution Time-of-Flight Aerosol Mass Spectrometer (HR-ToF-AMS), and coating thickness determined by the optical diameter method of rBC-containing particles with $D_{me,rBC}$ = 80 nm (black), with error bars denoting one standard deviation. Shaded regions delineate episodes A and B as in Figure 1.

rBC with a thin coating centered around $D_{me,rBC}$ = 200 nm and the other those that contain smaller amounts of rBC with a thick coating. Similar mixtures of fresh and aged rBC have been observed before [*Subramanian et al.*, 2010]: however, the negative lagtimes that are observed in episode B (Figure 3b) are unexpected and have not previously been reported. More than 60% of the sampled particles exhibited negative lagtimes at the peak of this episode. As negative

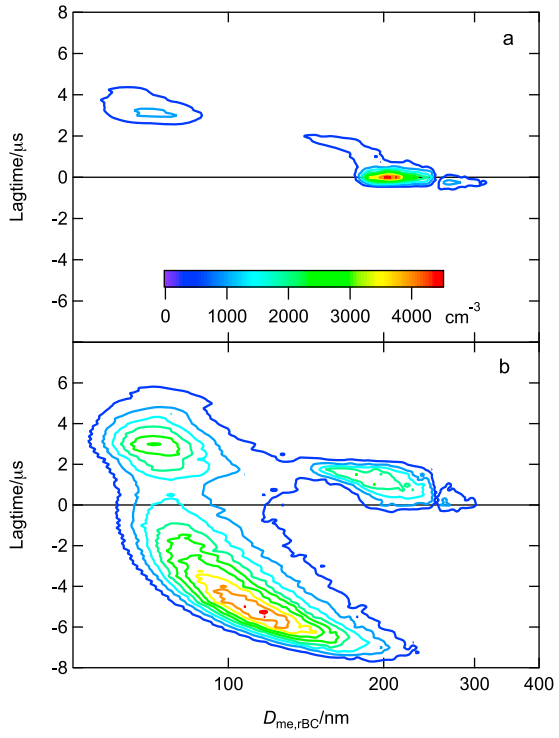

Figure 3. Lagtimes for (a) episode A and (b) episode B over time intervals shown by shaded regions in Figure 1 as a function of rBC mass-equivalent diameter $D_{me,rBC}$.

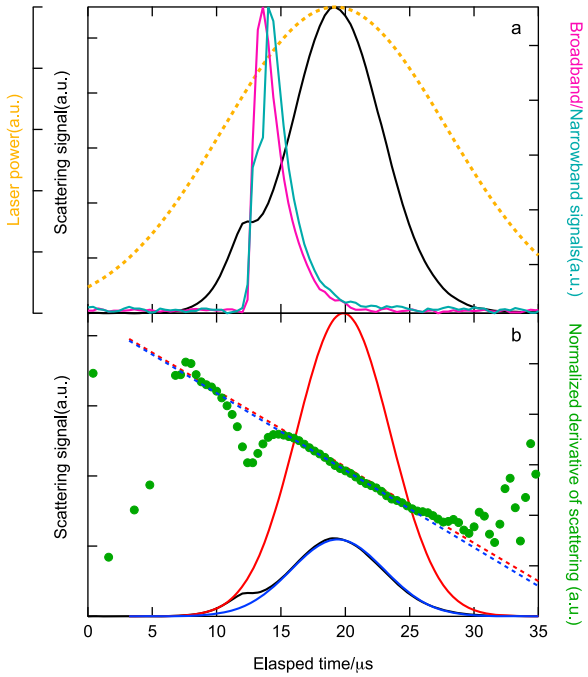

Figure 4. (a) Scattering signal (black line) and broadband (purple) and narrowband (teal) incandescence signals from a representative rBC-containing particle sampled in episode B, and laser intensity experienced by the particle (gold line). (b) The same scattering signal (black line) along with the normalized derivative of the scattering signal (green dots) and the best linear fits to the first (red dashed line) and second (blue dashed line) scattering peaks. Reconstructed Gaussian signals for the first (red line) and second (blue line) scattering peaks using the normalized derivative method are also shown. All signals are in arbitrary units (a.u.).

lagtimes in the conventional core-shell model would suggest that the rBC is incandescing *before* the coating is removed, their existence implies that this conceptual model does not accurately describe these particles.

[10] Scattering and incandescence signals representative of those particles with lagtimes in the range of $\Delta\tau = -1.25$ to -8 μs are shown in Figure 4a. The observed negative lagtimes are due to the maximum amplitude of the scattering signal occurring *after* that of the incandescence signal. It is the existence of the two scattering peaks and their position relative to the incandescence signal that yield new physical insight into the microphysical structure of the sampled particles. The first scattering peak is closely followed by a decrease in the scattering signal that is nearly simultaneous with the appearance of rBC incandescence. A second scattering peak then occurs with greater amplitude than the first. Particle coincidence can be eliminated as the cause of the multiple peaks by the relatively low number concentrations of particles measured by the SP2 (200–300 cm^{-3}) and by the asymmetry in the distribution of lagtimes (Figure 3b). Similarly, instrument artifact can be eliminated as a second SP2 deployed during this campaign observed similar behavior in the scattering signal.

[11] The temporal behavior of the scattering signals was examined using the normalized derivative method [*Moteki and Kondo*, 2008] in which the time derivative of the logarithm of the scattering amplitude (i.e., the time derivative of

the scattering amplitude divided by the scattering amplitude itself) is plotted as a function of time. The normalized derivative of a Gaussian signal, such as that resulting from a particle of constant diameter passing through the Gaussian laser beam in the SP2 at constant velocity, will be a linear function of time with slope and intercept depending only on the linewidth of the laser beam and particle velocity. Deviation from linearity indicates a change in diameter of the particle, such as would occur during evaporation. Application of this technique to the scattering signal shown in Figure 4a reveals that the leading edge of the first scattering peak exhibits a Gaussian behavior with time as does the second scattering peak, as demonstrated by the linearity of the normalized derivative of the scattering signal over these regions (Figure 4b). These results indicate that there is no loss of coating material occurring during these times. For the leading edge of the first scattering signal this is not surprising, as the rBC has not yet absorbed sufficient energy to produce appreciable evaporation of the coating. However, the existence of a scattering signal *after* rBC incandescence is unexpected, as it has traditionally been thought that incandescence would occur only after coating material has evaporated. Furthermore, the amplitude of the second scattering peak is considerably greater than that of the first. Reconstruction of the expected scattering signal for the particle (Figure 4b) using the leading edge of the first scattering peak results in an amplitude that is larger than that measured for the second peak, consistent with loss of rBC through incandescence. These observations suggest a mechanism in which both rBC without coating material and coating material without rBC can simultaneously co-exist in the laser beam. This study reports, for the first time, such behavior for ambient particles.

[12] In a laboratory study using the SP2, *Moteki and Kondo* [2007] observed a bimodal scattering signal resulting from particles consisting of graphite with very thick (>200 nm) coatings of glycerol and oleic acid, with both peaks of roughly equal amplitude (thinner coating resulted in typical behavior of scattering followed by incandescence). The maximum of the first scattering peak coincided with the onset of rBC incandescence and the second scattering signal occurred after the incandescence signal (similar to what is observed here). To explain their observations, these investigators postulated that the particles underwent an explosive event brought about by the inability of the coating material to dissipate heat sufficiently rapidly through evaporation.

[13] It is proposed here that an analogous fragmentation occurs for the particles observed in the present ambient data set. Such a mechanism could explain the presence of two scattering signals: the first caused by the initial particle consisting of rBC with coating and the second from the coating alone. Particle fragmentation would also explain why the amplitude of the second peak is smaller than that of the scattering signal reconstructed from the leading edge of the first peak, the causes being the smaller particle size and the change in the index of refraction due to the absence of rBC (calculations demonstrate that the contribution of these factors to the decrease in amplitude may be of comparable magnitude).

[14] Despite the similarities between the behavior of thickly coated rBC particles in the laboratory and the present observations, there exist two important differences. First, the reported fragmentation of laboratory-generated particles occurred only for large coating thicknesses (~200–300 nm), much greater than thicknesses observed here (<100 nm). Second, the amplitudes of the scattering peaks shown in Figure 16 of *Moteki and Kondo* [2007] were roughly equal, suggesting that the rBC-containing particle traveled farther into the laser beam as a single particle before fragmentation. In contrast, the ambient particles considered here exhibit scattering signals for which the amplitude of the first peak is much smaller than that of the second peak implying that particle fragmentation occurs soon after entry into the laser beam. It is proposed that these differences are due to rBC being located very near the surface in the ambient rBC-containing particles, whereas the laboratory particles possessed structures that more closely resembled a core-shell configuration. The particles in episode A exhibited only positive lagtimes indicative of coating evaporation followed by rBC incandescence implying that these particles also possess structures that more closely resemble a core-shell configuration. In contrast, the existence of negative lagtimes for particles in episode B implies a qualitative structural difference between these particles and those in episode A, and therefore a core-shell model does not provide an accurate description of these particles.

[15] Although no accompanying microscopy analysis was available during the measurement campaign, support for the above inference of near-surface rBC is provided by a recent TEM analysis of organic-coated soot collected in Mexico City [*Adachi et al.*, 2010]. These investigators reported that the soot analyzed was likely to be located near the surface of the particle. The mechanism for generation of near-surface soot proposed by those investigators involved condensation of organic material onto nascent soot that effectively froze the aggregate in an uncollapsed form, followed by preferential growth of coating on the more organic portion of the particle. It is likely that a similar mechanism is responsible for the current results in episode B.

[16] One of the unique contributions of the present analysis is the ability to distinguish particles containing rBC in which the rBC is near the surface from those for which the structure is more like a core-shell configuration by the consideration of the lagtime between the peaks of the scattering and incandescence signals. Furthermore, this approach can be used to investigate aerosol processes by examining the fraction of particles, Φ_{ns} with lagtimes $\Delta\tau < -1.25$ μs (this value is used rather than zero to allow for uncertainties in lagtime determination). For example, application of this technique to the current data set (Figure 5a) reveals that Φ_{ns} remained near 15% during the early part of the day on August 2, 2011, including the time characterized by episode A, and rapidly increased to greater than 60% with the onset of episode B, later decreasing in a similar manner to the organic aerosol mass concentration. Preliminary analysis of other days during this campaign indicates that Φ_{ns} typically hovered around 10%. The HR-ToF-AMS analysis (Figure 2) indicates that the organic aerosol in episode B is aged, as evidenced by an O:C ratio approaching 0.50. Three-day HYSPLIT back-trajectory calculations (R. R. Draxler and G. D. Rolph, HYSPLIT (HYbrid Single-Particle Lagrangian Integrated Trajectory) Model, 2011, http://ready.arl.noaa.gov/HYSPLIT.php) reveal that the air sampled on August 2 followed a southeast transect from south-central Canada, where the Canadian Wildland Fire Information System (CWFIS, 2011, http://maps.nofc.cfs.nrcan.gc.ca/cwfisapps/interactivemap/index.phtml#) reported several wildfires east

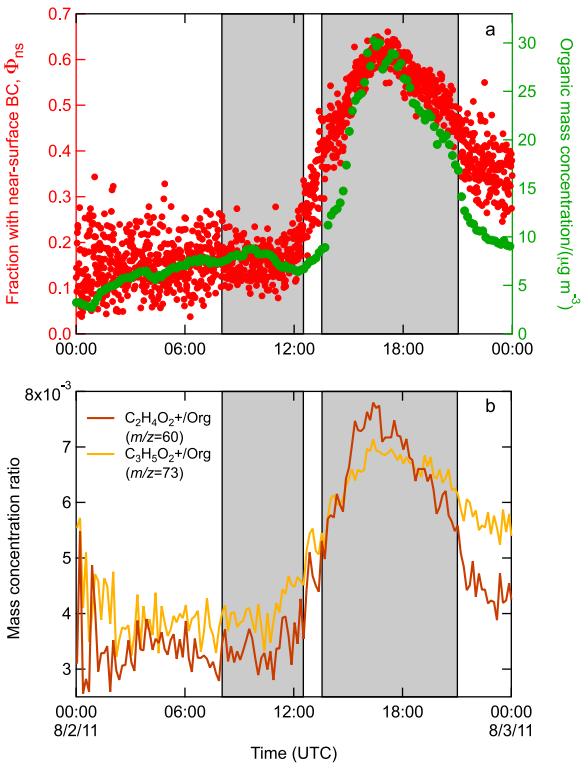

Figure 5. (a) Fraction of near-surface rBC-containing particles, Φ_{ns} (red dots), and organic aerosol mass concentration determined by HR-ToF-AMS (green dots). (b) Ratio of the mass concentrations of biomass burning tracers $C_2H_4O_2^+$ (m/z = 60) and $C_3H_5O_2^+$ (m/z = 73) to total mass concentration of organics determined by HR-ToF-AMS. Shaded regions delineate episodes A and B as in Figure 1.

of Lake Winnipeg and into western Ontario on July 30. In addition, the HR-ToF-AMS mass spectra show elevated signals of tracer ions for biomass burning organic aerosols [*Alfarra et al.*, 2007] (m/z = 60 (primarily $C_2H_4O_2^+$) and m/z = 73 (primarily $C_3H_5O_2^+$)), relative to organics (Figure 5b) during episode B but not during episode A. It is to be noted that episode A is likely associated with urban transport as evidenced by the presence of $C_4H_9^+$ (m/z 57) and that no biomass burning tracers were observed in this air mass. These results indicate that the particles exhibiting negative lagtimes, and hence containing near-surface rBC, likely derive from biomass burning events and that these particles were formed through condensation of organic substances onto rBC. One intriguing question posed by the present result is whether the occurrence of near-surface rBC particles is uniquely associated with biomass burning. Given that an estimated 40% of BC emissions originate from biomass burning events [*Ramanathan and Carmichael*, 2008; *Bond et al.*, 2004], the answer to this question could have wide-ranging impact which will be explored in future publications.

[17] Detailed information provided on particle morphology has important implications for reducing the uncertainty in BC direct forcing. Particles with rBC located near the surface will exhibit less lensing-induced light absorption enhancement than those coated rBC particles whose structure more closely resembles the idealized core-shell configuration, as originally argued by Fuller and coworkers [*Fuller et al.*, 1999, and references therein] and most recently reemphasized by Buseck and co-workers [*Adachi et al.*, 2010, 2011; *Freney et al.*, 2010]. These latter investigators, using a discrete dipole approximation, estimated that particles in Mexico City with near-surface soot would exhibit a 20% reduction in their contribution to direct radiative forcing over that calculated using a core-shell model [*Adachi et al.*, 2010]. The variability in the fraction of near-surface rBC particles observed in the present study may thus have consequences for calculation of the direct forcing by BC.

4. Conclusion

[18] The presence of negative lagtimes for rBC-containing particles measured by the SP2, i.e., scattering occurring *after* rBC incandescence, has been observed in ambient particles and is reported here for the first time. Negative lagtimes may be dominant in some situations: in one biomass burning plume more than 60% of the rBC-containing particles exhibited this behavior. Examination of the scattering signal using the normalized derivative method indicates that this scattering was caused by a particle that did not contain rBC. This observation is explained by rBC being located near the surface of the initial particle. As a result, energy from the SP2 laser that is absorbed by the rBC is not dissipated by evaporation of a uniform core, as is typically assumed for core-shell configurations, but rather fragmentation of the rBC from the remaining non-absorbing material occurs. Such an explanation also accounts for the observations of two scattering signals, one from the initial rBC-containing particle and the other from the particle consisting of only the non-absorbing material, as well as the asymmetry of the amplitudes of these two signals.

[19] The lagtime technique described above permits real-time analysis of rBC-containing particle structure and provides a way to distinguish those rBC-containing particles for which rBC is near the surface from those more closely resembling the conventional core-shell configuration. Additionally, this technique provides quantification of the fraction of near-surface rBC particles among all ambient rBC-containing particles, and thus yields insight into the processes of aerosols containing these particles. These observations suggest that the core-shell model is not applicable to all rBC-containing particles (see, e.g., *Adachi et al.* [2010, 2011] and *Freney et al.* [2010, and references therein] for TEM observations of non-spherical aerosols in a wide range of locations). Furthermore, the occurrence of a large fraction of near-surface rBC particles has implications for radiative forcing calculations in which the core-shell model is assumed. The observations reported here suggest several lines of inquiry, such as the effect of the location of rBC within the particles on mass absorption cross section, determination of whether the existence of near-surface rBC is indicative of or unique to biomass burning aerosols, and comparisons with microscopy.

[20] **Acknowledgments.** The authors wish to thank R. Subramanian (DMT) for several discussions on the subtle inner workings of the SP2, Shan Zhou (UCD) for assisting in AMS data analysis, and Danielle Weech (UIUC) for running the HYSPLIT calculations. We gratefully acknowledge the Atmospheric Science Program within the Office of Biological and Environmental Research of DOE for supporting field and analysis activities and the Atmospheric Radiation Measurement (ARM) program for the SP2. This

research was performed under sponsorship of the U.S. DOE under contracts DE-AC02-98CH10886 and DE-FG02-11ER65293. The authors thank two anonymous reviewers for their assistance in evaluating this paper.

[21] The Editor thanks two anonymous reviewers for their assistance in evaluating this paper.

References

Ackerman, T. P., and O. B. Toon (1981), Absorption of visible radiation in atmosphere containing mixtures of absorbing and nonabsorbing particles, *Appl. Opt.*, *20*, 3661–3670, doi:10.1364/AO.20.003661.

Adachi, K., S. H. Chung, and P. R. Buseck (2010), Shapes of soot aerosol particles and implications for their effects on climate, *J. Geophys. Res.*, *115*, D15206, doi:10.1029/2009JD012868.

Adachi, K., E. Freney, and P. R. Buseck (2011), Shapes of internally mixed hygroscopic aerosol particles after deliquescence, and their effect on light scattering, *Geophys. Res. Lett.*, *38*, L13804, doi:10.1029/2011GL047540.

Alfarra, M. R., et al. (2007), Identification of the mass spectral signature of organic aerosols from wood burning emissions, *Environ. Sci. Technol.*, *41*(16), 5770–5777, doi:10.1021/es062289b.

Bond, T. C., and R. W. Bergstrom (2006), Light absorption by carbonaceous particles: An investigative review, *Aerosol Sci. Technol.*, *40*, 27–67, doi:10.1080/02786820500421521.

Bond, T. C., D. G. Streets, K. F. Yarber, S. M. Nelson, J.-H. Woo, and Z. Klimont (2004), A technology-based global inventory of black and organic carbon emissions from combustion, *J. Geophys. Res.*, *109*, D14203, doi:10.1029/2003JD003697.

Cross, E. S., et al. (2010), Soot particle studies—Instrument intercomparison—Project overview, *Aerosol Sci. Technol.*, *44*(8), 592–611, doi:10.1080/02786826.2010.482113.

Forster, P. et al. (2007), Changes in atmospheric constituents and in radiative forcing, in *Climate Change 2007: The Physical Science Basis. Contribution of Working Group I to the Fourth Assessment Report of the Intergovernmental Panel on Climate Change*, edited by S. Solomon et al., pp. 129–234, Cambridge Univ. Press, Cambridge, U. K.

Freney, E., K. Adachi, and P. R. Buseck (2010), Internally mixed atmospheric aerosol particles: Hygroscopic growth and light scattering, *J. Geophys. Res.*, *115*, D19210, doi:10.1029/2009JD013558.

Fuller, K. A., W. C. Malm, and S. M. Kreidenweis (1999), Effects of mixing on extinction by carbonaceous particles, *J. Geophys. Res.*, *104*(D13), 15,941–15,954, doi:10.1029/1998JD100069.

Jacobson, M. Z. (2001), Strong radiative heating due to the mixing state of black carbon in atmospheric aerosols, *Nature*, *409*, 695–697, doi:10.1038/35055518.

Moteki, N., and Y. Kondo (2007), Effects of mixing state on black carbon measurements by laser-induced incandescence, *Aerosol Sci. Technol.*, *41*(4), 398–417, doi:10.1080/02786820701199728.

Moteki, N., and Y. Kondo (2008), Method to measure time-dependent scattering cross-sections of particles evaporating in a laser beam, *J. Aerosol Sci.*, *39*, 348–364, doi:10.1016/j.jaerosci.2007.12.002.

Pósfai, M., and P. R. Buseck (2010), Nature and climate effects of individual tropospheric aerosol particles, *Annu. Rev. Earth Planet. Sci.*, *38*, 17–43, doi:10.1146/annurev.earth.031208.100032.

Ramanathan, V., and G. Carmichael (2008), Global and regional climate changes due to black carbon, *Nat. Geosci.*, *1*, 221–227, doi:10.1038/ngeo156.

Schwarz, J. P., et al. (2006), Single-particle measurements of midlatitude black carbon and light-scattering aerosols from the boundary layer to the lower stratosphere, *J. Geophys. Res.*, *111*, D16207, doi:10.1029/2006JD007076.

Schwarz, J. P., et al. (2010), The detection efficiency of the single particle soot photometer, *Aerosol Sci. Technol.*, *44*, 612–628, doi:10.1080/02786826.2010.481298.

Subramanian, R., et al. (2010), Black carbon over Mexico: The effect of atmospheric transport on mixing state, mass absorption cross-section, and BC/CO ratios, *Atmos. Chem. Phys.*, *10*, 219–237, doi:10.5194/acp-10-219-2010.

L. Kleinman, E. R. Lewis, and A. J. Sedlacek III, Atmospheric Science Division, Brookhaven National Laboratory, Bldg. 815E, Upton, NY 11973, USA. (sedlacek@bnl.gov)

J. Xu and Q. Zhang, Department of Environmental Toxicology, University of California, 4251A Meyer Hall, Davis, CA 95616, USA.